Ecological Engineering & Environmental Technology, 2025, 26(11), 204–216 https://doi.org/10.12912/27197050/211865 ISSN 2719–7050, License CC-BY 4.0

Geophysical assessment of liquefaction hazards and environmental implications in Pidie Jaya, Indonesia

Muhammad Syukri^{1,2*}, Zul Fadhli², Haris Saputra³, Rini Safitri¹

- ¹ Department of Physics, Faculty of Sciences, Universitas Syiah Kuala, Banda Aceh, 23111, Indonesia
- ² Department of Geophysics Engineering, Faculty of Engineering, Universitas Syiah Kuala, Banda Aceh, 23111, Indonesia
- ³ Department of Civil Engineering, Faculty of Engineering, Universitas Muhammadiyah Aceh, Banda Aceh, 23123, Indonesia
- * Corresponding author's e-mail: m.syukri@usk.ac.id

ABSTRACT

Liquefaction is a significant geohazard in seismically active regions, causing ground deformation, infrastructure damage, and agricultural disruption. This study aims to assess the liquefaction susceptibility of sediments in Pidie Jaya, Aceh, Indonesia, and evaluate their environmental implications through an integrated geophysical approach combining electrical well logging and two-dimensional (2D) electrical resistivity tomography (ERT). Surveys were conducted in Rhieng Krueng, Dayah Baroh, and Jurong Ara, where borehole logging provided vertical stratigraphy and resistivity data, while 2D ERT sections revealed lateral variability. The results indicate heterogeneous subsurface sequences consisting of sand $(0-57 \Omega m)$, sandy clay $(0-32 \Omega m)$, and clay $(13-750 \Omega m)$, with loose, water-saturated sands confined between impermeable clay layers forming aquifers highly prone to liquefaction. Shallow groundwater depths, averaging 6.8 m, further exacerbate the risk of excess pore-pressure buildup during seismic shaking. These findings highlight critical horizons where soil instability may endanger agricultural productivity, irrigation systems, and rural settlements. However, the research is limited to three survey sites, which may not fully capture the district's spatial variability, and integration with geotechnical and seismic response analyses is recommended. The practical contribution of this work lies in demonstrating that combining electrical logging and ERT provides a reliable, cost-effective framework for identifying liquefaction-prone sediments and evaluating hydrogeological conditions. This integrative method offers valuable insights for disaster risk reduction, land-use planning, and resilient infrastructure development. As one of the first studies applying this approach to Pidie Jaya, it underscores the environmental significance of subsurface heterogeneity and provides essential input for sustainable hazard mitigation in seismically active regions.

Keywords: liquefaction, electrical well logging, resistivity, rural area, environmental monitoring.

INTRODUCTION

Liquefaction phenomena can induce severe impacts, including ground subsidence, surface cracking, landslides, and damage to public infrastructure (Jefferies and Been, 2015). A notable example is the 26 December 2004 Aceh and Nias earthquake (Mw 9.3), which triggered liquefaction in urban areas of Banda Aceh, causing extensive structural damage due to weakened loadbearing capacity in alluvial plains along coastal areas and the Krueng Aceh River (Syukri et al.,

2020b; Rusydy et al., 2022; Irhami, et al., 2023). Similarly, liquefaction following the 2018 Palu-Donggala earthquake transformed landslide material into debris flows over gentle slopes (~2%), reaching distances over 800 meters (Kusumawardani et al., 2021).

Received: 2025.09.21

Accepted: 2025.10.20

Published: 2025.11.01

On 6 December 2016, a Mw 6.5 earthquake struck Pidie Jaya, Aceh, approximately 30 km north of the Sumatran Fault (BMKG, 2016). This shallow earthquake caused more than 100 fatalities and destroyed over 10,000 structures (ReliefWeb, 2016). The event was associated

with strike-slip movement along the Samalan-ga-Sipopok Fault, oriented southwest-northeast (BMKG, 2016; Muzli et al., 2018; Qodri et al., 2022). The region falls within seismic zone 3 and consists of Quaternary deposits, including fluviatile sediments, alluvium, and coastal embankments (Bennett et al., 1981), which are vulnerable to liquefaction. Such deposits, composed of granular, water-saturated, low-density sediments, are highly susceptible to deformation under seismic loading, especially where shallow groundwater tables exist (Anda et al., 2024).

Various methods have been employed globally to assess liquefaction susceptibility. Shear wave velocity (Vs) measurements help predict liquefaction potential and emphasize the importance of local topography for soil stability (Asmirza et al., 2019). Standard Penetration Test (SPT) data identify sand layers as critical factors for liquefaction risk, particularly in shallow groundwater areas (Munirwan et al., 2020). Electrical logging, combined with Swedish weight-sounding (SWS) and SPT, has been successfully applied in Japan to delineate liquefaction-prone zones (Sako and Fujii, 2019). Electrical Resistivity Tomography (ERT) provides high-resolution lateral imaging of subsurface resistivity, identifying saturated zones with low resistivity (0.1–10 Ω m) that are prone to liquefaction (Syukri et al., 2020; Amoroso et al., 2020; Duan et al., 2023).

Given these capabilities, this study integrates electrical logging and 2D ERT to assess lique-faction potential in Pidie Jaya, Aceh. Electrical logging provides detailed in situ vertical measurements of soil properties, while ERT captures lateral variations, enabling detection of aquifers, water-saturated layers, and unconsolidated sediments that are susceptible to liquefaction (Kim et al., 2023; Lee et al., 2023; Ayadat, 2021; Ray and Sahu, 2021).

This study provides a high-resolution, integrated evaluation of liquefaction-prone sediments in a seismically active region with recurrent earthquake hazards. Mapping the spatial distribution of vulnerable layers, groundwater levels, and subsurface structures is critical for disaster risk reduction, sustainable land-use planning, and resilient infrastructure design in Pidie Jaya. The integration of electrical logging and ERT represents an advancement over single-method approaches, offering multidimensional data to predict liquefaction impacts and mitigate environmental and socio-economic risks (Rastogi et al., 2022)

This study aims to investigate liquefaction-susceptible sediments in Pidie Jaya, Aceh, by integrating electrical well logging and 2D resistivity imaging. The objectives are to characterize the subsurface lithology, identify unconsolidated and water-saturated layers prone to liquefaction, evaluate the spatial distribution and hydrogeological conditions of these sediments, and assess their potential environmental implications for agriculture, settlements, and infrastructure. By combining these geophysical methods, the study seeks to provide a comprehensive understanding of liquefaction hazards in the region and support sustainable land-use and disaster risk management strategies.

GENERAL GEOLOGY OF STUDY AREA

Based on the geological map of Pidie Jaya compiled by Bennett et al. (1981), the study area exhibits diverse geological formations, including alluvial, volcanic, and sedimentary rock types (Figure. 1). The coastal plain of Pidie Jaya Regency is dominated by Quaternary alluvial deposits (Qh), composed mainly of unconsolidated sand, silt, and clay, which are highly susceptible to liquefaction under seismic loading. In contrast, the central part of the Bukit Barisan Mountains is occupied by more consolidated igneous rocks such as diorite, granite, gabbro, and schist, while the slopes are dominated by sedimentary formations including conglomerates, breccias, and lava flows. Surrounding units, such as the Olim Volcanics (Qvo) and Meucampi Formation (Tlm), provide a contrasting geological framework that is more resistant to liquefaction compared to the unconsolidated coastal alluvium.

The tectonic setting of Pidie Jaya further amplifies its vulnerability. A Mw 6.5 earthquake in 2016 activated a previously unknown fault system west of the structures responsible for the Mw 6.1 event in 1967, suggesting either a separate fault or an extension of an older one (Muzli et al., 2018). These seismic events highlight the dynamic nature of the region, located near the Sumatran Fault Zone, and emphasize the importance of detailed subsurface characterization. In this context, the integration of electrical well logging and 2D resistivity imaging provides essential insights into the thickness, lithological variability, and groundwater conditions of the alluvial deposits, allowing for the identification of

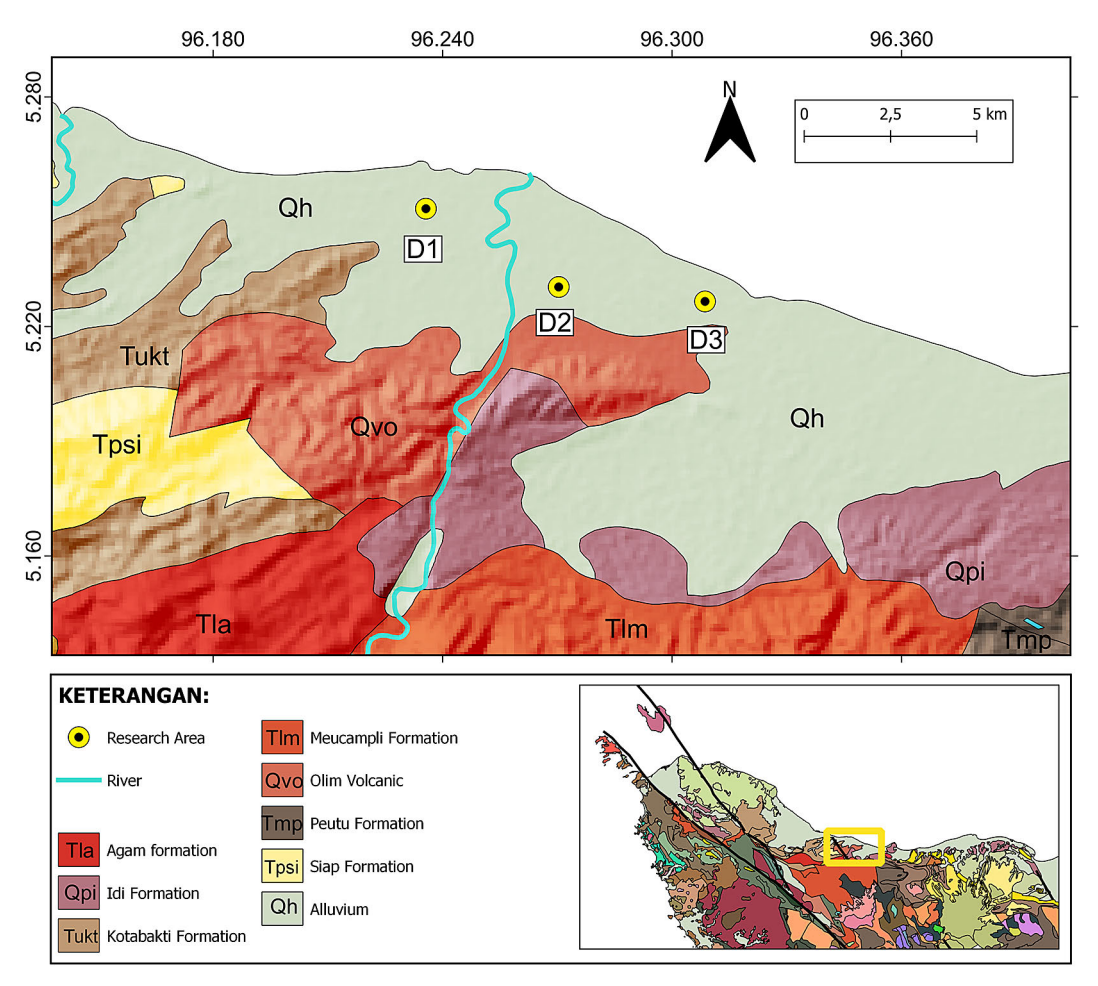


Figure 1. Regional geological map of Pidie Jaya (modified from Bennett et al., 1981)

liquefaction-prone sediments and their environmental implications for urban development and disaster mitigation in Pidie Jaya.

METHODOLOGY

The geophysical survey in Pidie Jaya District was conducted at three locations: Rhieng Krueng Village (Meureudu Subdistrict), Dayah Baroh Village (Ulim Subdistrict), and Jurong Ara Village (Jangka Buya Subdistrict). At each site, two-dimensional electrical resistivity tomography (2D ERT) profiles were established along a northwest–southeast orientation with a total line length of 336 meters. Electrical well logging was performed at selected boreholes, reaching depths of up to 120 meters, to complement the 2D ERT surveys and provide high-resolution vertical characterization of subsurface sediments, particularly liquefaction-prone units.

In Rhieng Krueng (D1) and Jurong Ara (D3), boreholes were located approximately 20–35

meters from the corresponding ERT profiles (R1 and R3), whereas at Dayah Baroh (D2), the borehole was nearly aligned with the ERT survey (R2) with an offset of 115 meters (Figure 2). Data acquisition was conducted with support from the Aceh Energy and Mineral Resources Department and followed standard procedures, including site selection, recording of coordinates, elevation, and environmental conditions. For ERT, an ARES resistivity meter was used, deploying current and potential electrodes along the survey line, while borehole probes were lowered at 1-meter intervals until the maximum depth was reached (Reynolds, 2011).

Electrical resistivity tomography (ERT)

Data acquisition

ERT measurements were carried out along three survey lines (R1–R3) using the Wenner–Schlumberger array with a 6-meter electrode spacing and a total line length of 336 meters, as illustrated

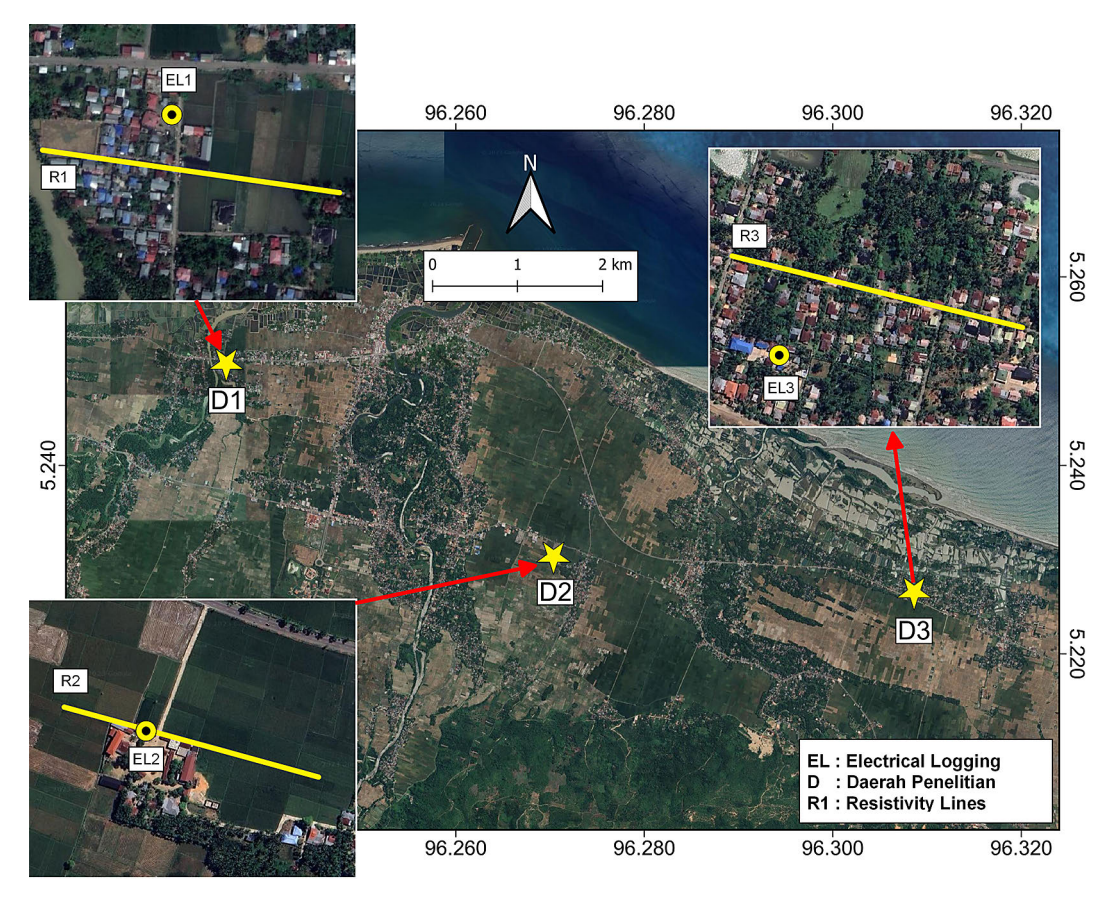


Figure 2. Map of the study area

in Figure 3. The measurements were performed using an ABEM Terrameter SAS 4000 integrated with a multi-electrode system. This array configuration provides an optimal balance between depth of investigation and lateral resolution (Loke, 2004; Dahlin and Zhou, 2004). A total of 57 electrodes were deployed, enabling an interpretation depth of approximately 60 meters, depending on subsurface resistivity and ground conductivity. During the survey, electric current was injected through the current electrodes, while potential differences were measured across potential electrodes to obtain apparent resistivity values.

Data processing

Resistivity data were processed using RES-2DINV software. Initial processing included quality checks to identify noise and outliers, removing data with errors above 5%. Numerical inversion was performed using the least-squares method until RMS error fell below 10%. Inversion parameters, such as smoothness and iteration number, were adjusted according to local geological conditions to improve accuracy, as shown in Figure 4.

Interpretation

The 2D resistivity sections illustrate lateral and vertical resistivity variations. Low resistivity zones correspond to clay or water-saturated sand, moderate resistivity to loose sand, and high resistivity to gravel or compacted layers. These interpretations form the basis for identifying liquefaction-prone zones.

Electrical well logging

Data acquisition

The well-logging data used in this study were obtained from the Aceh Department of Energy and Mineral Resources (ESDM), which conducted the original field acquisition as part of a regional subsurface investigation program. Therefore, the authors did not perform direct field measurements but utilized the official dataset provided by the agency for scientific analysis and interpretation.

The original data acquisition by the ESDM team followed standard geophysical well-logging protocols as outlined by Reynolds (2011). The procedure involved determining borehole

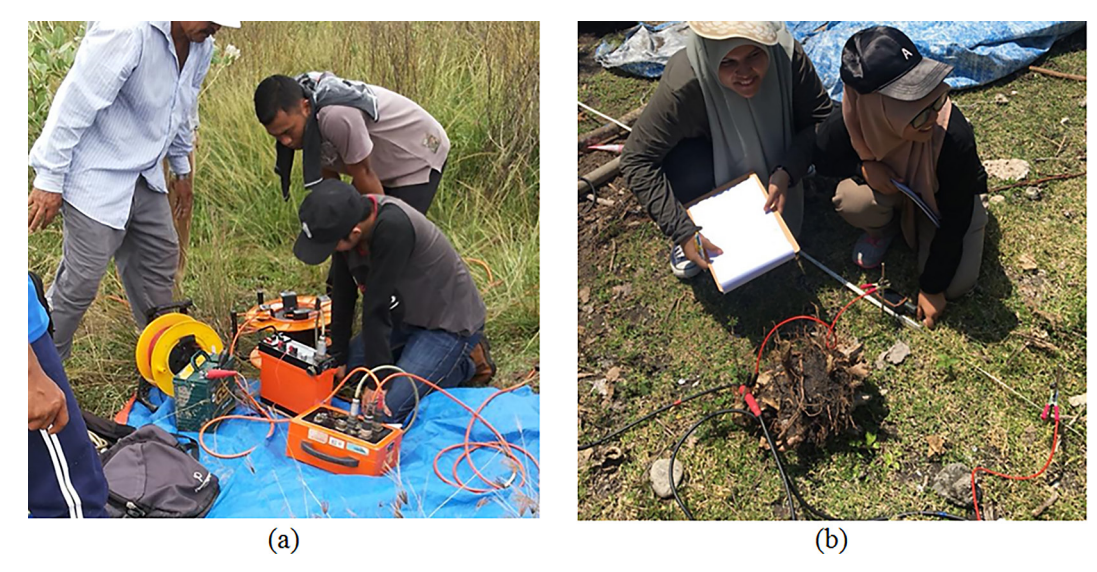


Figure 3. Field setup during 2D resistivity data acquisition using an ABEM Terrameter SAS 4000 multi-electrode resistivity system: (a) instrument setup and cable connection, (b) electrode installation and potential measurement

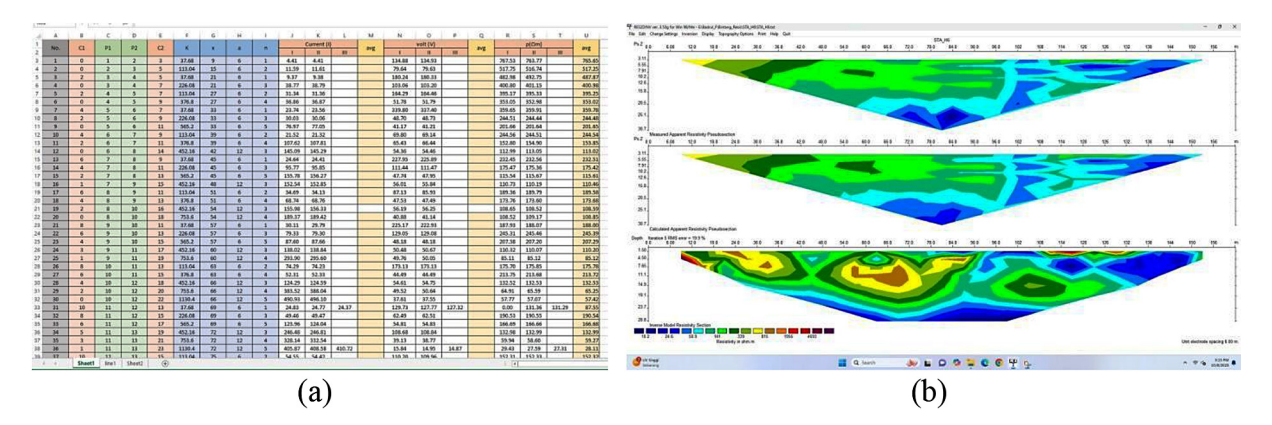


Figure 4. Data Processing: (a) raw field resistivity data obtained from the Terrameter SAS 4000 system, b) the 2D resistivity processing workflow using RES2DINV software, showing from top to bottom: measured apparent resistivity pseudosection, calculated apparent resistivity pseudosection, and the final inverse model resistivity section illustrating the interpreted subsurface layers

coordinates, elevations, and surface conditions prior to measurement. At each site, a Naniura ND 112P resistivity logging system was installed. The potential and current electrodes were positioned on the surface, while the borehole electrode – connected via a signal cable – was lowered incrementally at 1-meter intervals from the surface to the maximum borehole depth. During each interval, resistivity readings in Resistivity 16 mode and spontaneous potential (SP) values were recorded in field sheets. These measurements were later digitized by the ESDM team and archived in their geophysical database.

The dataset provided to this study included the raw resistivity and SP values, borehole

coordinates, depth intervals, and lithological information derived from drilling cuttings. This ensured that the analysis maintained high accuracy and traceability while minimizing potential duplication of field activities.

Data processing

Processing of the electrical logging and cutting data was performed using LogPlot 2003 software. The purpose was to produce one-dimensional (1D) resistivity profiles illustrating variations in subsurface lithology with depth.

The workflow began by launching LogPlot 2003 in single-user mode, followed by designing the layout for data visualization. The layout

included static text headers (title, coordinates, and location), scale bars, lithology columns, and resistivity curves (16" and 64"). After finalizing the design, it was saved in.ldf format for later use.

Depth parameters were defined (start = 0 m, end = maximum borehole depth), and resistivity log data were entered using the Crossplot Curves function—assigning Curve 1 to Resistivity 16" and Curve 2 to Resistivity 64". Lithological data from drilling cuttings were input using the Lithology menu, and descriptive annotations were added for each layer (e.g., aquifer, aquiclude). The compiled dataset was saved in dat format and visualized using the Compile a Log function. The final logs were annotated using Microsoft Word for clarity and labeling of key stratigraphic boundaries.

Interpretation

The vertical resistivity profiles from borehole logging revealed distinct subsurface lithological variations. Low resistivity zones (<20 Ω m) correspond to clay or silty layers, moderate resistivity (20–60 Ω m) indicates water-saturated sand, while high resistivity (>60 Ω m) represents gravel or coarse sand formations. The integrated interpretation of borehole and ERT data enhanced both vertical and lateral resolution of subsurface structures. This combined approach enabled the identification of aquifer horizons and weak zones potentially susceptible to liquefaction.

Data integration

Integration of ERT and borehole data was conducted by correlating borehole logs with 2D resistivity sections. ERT provides lateral 2D information, while borehole logs give detailed 1D vertical profiles. Cross-validation reduces interpretational ambiguity, distinguishing between saturated clay and loose sand. The integrated results indicate that D1 (Rhieng Krueng) and D2 (Dayah Baroh) contain thick, water-saturated loose sand layers with moderate—low resistivity, showing high liquefaction potential. D3 (Jurong Ara) exhibits transitional conditions of saturated sand and clay.

Data integration was performed using RES-2DINV and RockWork16 to produce comprehensive subsurface correlation sections, following established methods (Loke and Barker, 1996; Binley and Kemna, 2005; Loke, 2010) that emphasize the combination of surface and borehole geophysical techniques.

RESULTS AND DISCUSSION

The processing of electrical well logging data produced one-dimensional profiles consisting of resistivity, lithology, and depth curves, which were analyzed using LogPlot 2003. These results were then correlated with the two-dimensional resistivity inversion models generated from RES-2DINV software. By integrating the well logging curves with 2D resistivity imaging, a more detailed characterization of the subsurface was obtained, particularly in relation to liquefaction-susceptible sediments.

The resistivity cross-sections (Figures 5–10) reveal that the near-surface deposits are dominated by low-resistivity values ranging from 1 to 20 Ω m, consistent with unconsolidated alluvial sediments such as sand and clay, often saturated with groundwater. These materials are highly susceptible to liquefaction due to their loose grain structure, low cohesion, and shallow groundwater table. At depths greater than 20–50 meters, zones with moderate resistivity values (20–100 Ω m) were detected, which correspond to interbedded sandstones of the Olim Formation and weathered volcanic deposits. These layers, although more compact, still allow for groundwater interaction, influencing the pore pressure regime.

The integration of electrical well logging with 2D resistivity imaging provides a more robust interpretation compared to single-method approaches. Well logging allows vertical control and accurate depth correlation of sedimentary layers, while resistivity imaging captures lateral heterogeneity across the survey lines. This combined approach highlights zones where groundwater saturation and unconsolidated sediments overlap, forming critical conditions for liquefaction during seismic events.

From an environmental perspective, the identification of liquefaction-prone layers is crucial for regional planning in Pidie Jaya. Liquefaction not only threatens infrastructure stability but also alters soil permeability, potentially affecting groundwater quality and land productivity. The findings therefore underscore the importance of integrating geophysical methods in hazard assessment and sustainable land-use planning in seismically active and environmentally vulnerable regions.

The integration of electrical well logging (EL1–EL3) and two-dimensional resistivity imaging (R1–R3) provides a detailed characterization

of the subsurface conditions in Pidie Jaya, revealing stratigraphic variations that significantly control liquefaction susceptibility.

Rhieng Krueng (EL1 and R1)

The EL1 drilled well, located at 5°15'02.90"N and 96°14'08.30"E in Rhieng Krueng Village, Meureudu District, reached a depth of 120 m and revealed three dominant lithologies: clay, sand, and gravel (Figure 5). Clay layers were identified at depths of 0–4 m, 10–44 m, 60–117 m, and 119–120 m, with resistivity values of 50–100 Ω m, indicating compact and relatively impermeable units. Sand horizons occurred at 50–60 m and 117–119 m, with resistivity values of 10–30 Ω m, reflecting unconsolidated, water-saturated materials. Gravel layers were encountered at 7–9 m and 43–50 m, with resistivity values of 30–50 Ω m, suggesting permeable zones that may serve as preferential pathways for groundwater flow.

The interbedding of sand and gravel with clay indicates heterogeneous subsurface conditions that strongly influence liquefaction susceptibility. Critical horizons include the shallow gravel at 7–9 m and the sand layer at 50–60 m, where seismic shaking may induce excess pore water pressure, reduce shear strength, and trigger liquefaction. These risks are further exacerbated by the shallow groundwater table in the area. From an environmental perspective, the alternation of permeable and impermeable strata not only controls liquefaction potential but also governs groundwater circulation and possible contamination pathways, which are vital for both hazard assessment and environmental management in Pidie Jaya.

The R1 resistivity profile, located east of the Krueng Beuracan River (Figure 6), reveals subsurface conditions dominated by sandy clay deposits with resistivity values of 20– $40~\Omega m$. A clay unit is identified along the first 40 m of the profile, exhibiting higher resistivity values (40– $200~\Omega m$) that suggest compact but relatively impermeable sediments. Beneath this layer, sand and gravel horizons are distributed at depths of 4–40 m, characterized by very low resistivity values ($<20~\Omega m$), reflecting unconsolidated, water-saturated materials.

The occurrence of saturated sand and gravel beneath a shallow clay cover indicates high liquefaction susceptibility during seismic events. Although the sandy clay provides partial cohesion, it cannot fully inhibit the buildup and

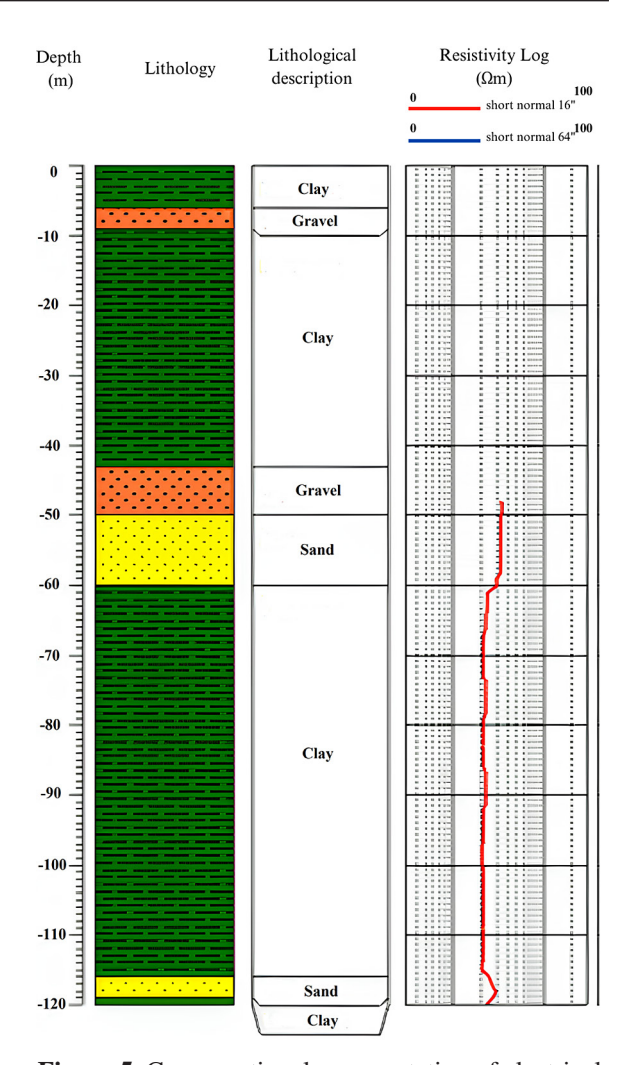


Figure 5. Cross-sectional representation of electrical logging data 1 (EL1) at point D1

upward migration of pore water pressure under strong ground shaking. Combined with shallow groundwater conditions, this stratigraphic configuration increases the risk of ground instability, subsidence, and surface cracking in Rhieng Krueng Village.

Dayah Baroh (EL2 and R2)

The drilled well EL2, located at $5^{\circ}13'49.20"N$ and $96^{\circ}16'13.30"E$ in Dayah Fathul Ainiyah Al-Aziziyah, Dayah Baroh Village, Ulim District, reached a depth of 119 m and revealed five lithological units: clay, sand, limestone, gravel, and sandy clay (Figure 7). Clay layers occur at shallow and deeper depths (0–4 m, 12–14 m, 43–45 m, 50-54 m, and 108-119 m), with resistivity values of 25-72 Ω m, representing relatively impermeable horizons. Sand dominates the succession at 4–12 m, 14-30 m, 36.5-43 m, and 91-108 m,

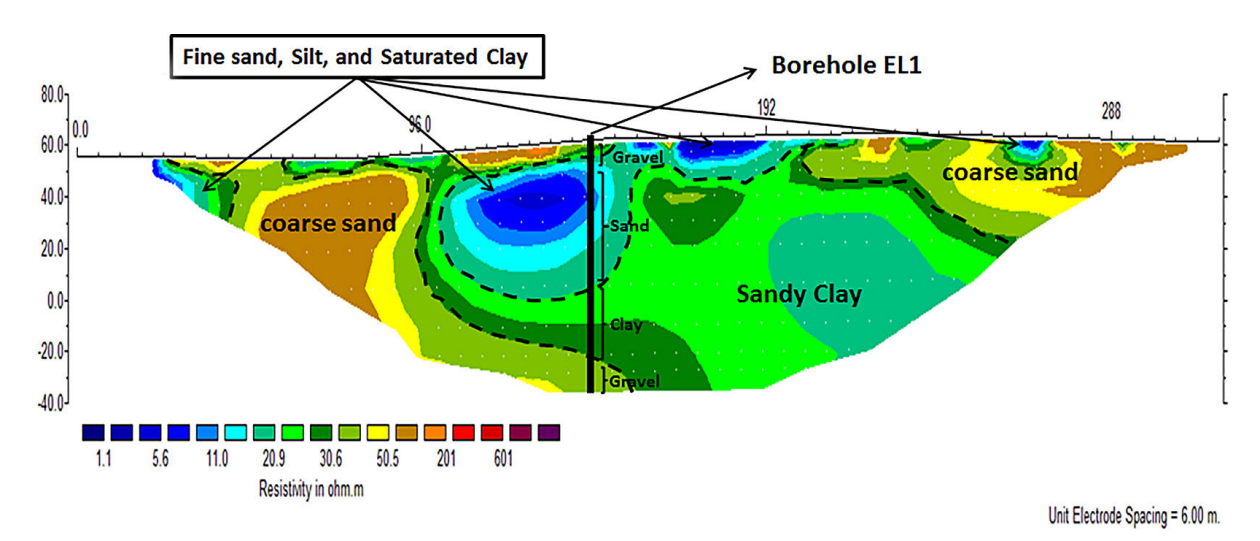


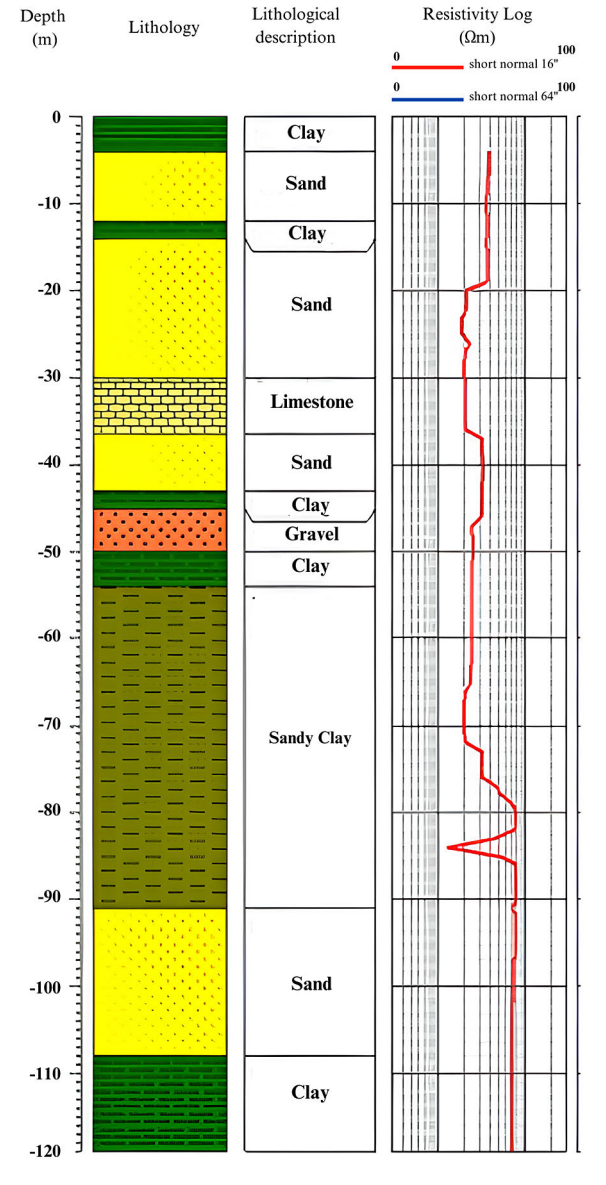
Figure 6. Cross-sectional representation of resistivity data 1 (R1) and electrical logging data 1 (EL1) at point D1

with resistivity values of 19–80 Ω m, indicating unconsolidated and potentially water-saturated sediments. A thin limestone bed is present at 30–36.5 m (20–21 Ω m), while a gravel unit occurs at 45–50 m (25–33 Ω m). Additionally, a thick sandy clay sequence extends from 54 to 91 m, showing resistivity values between 13 and 79 Ω m.

The subsurface profile reflects strong heterogeneity, with alternating sand, sandy clay, and gravel units interbedded with impermeable clay. Thick sand deposits at shallow depths (4–30 m), together with the intermediate sandy clay unit, highlight critical horizons prone to liquefaction under seismic loading. The generally low resistivity values also suggest substantial groundwater saturation, increasing the potential for excess pore pressure and soil strength reduction during earthquakes.

The resistivity line R2, located near the paddy field area (Figure 8), reveals a heterogeneous subsurface sequence. A clay layer dominates the shallow zone at 0–32 m with resistivity values of 32–180 Ω m, while coal and fine-grained sedimentary deposits occur at 4–30 m with very low resistivity (0–20 Ω m), indicating weakly consolidated and water-saturated strata. A sandy clay unit is present between 8–37 m (31–36 Ω m), and a gravel horizon is detected at 15–40 m with resistivity values of 13–82 Ω m.

The combination of loose sand, sandy clay, and gravel layers at shallow to intermediate depths suggests the presence of liquefaction-prone sediments. The low resistivity of coal-rich and fine sediments reflects high porosity and significant groundwater content, which under seismic



Figures 7. Cross-sectional representation of electrical logging data 2 (EL2) at point D2

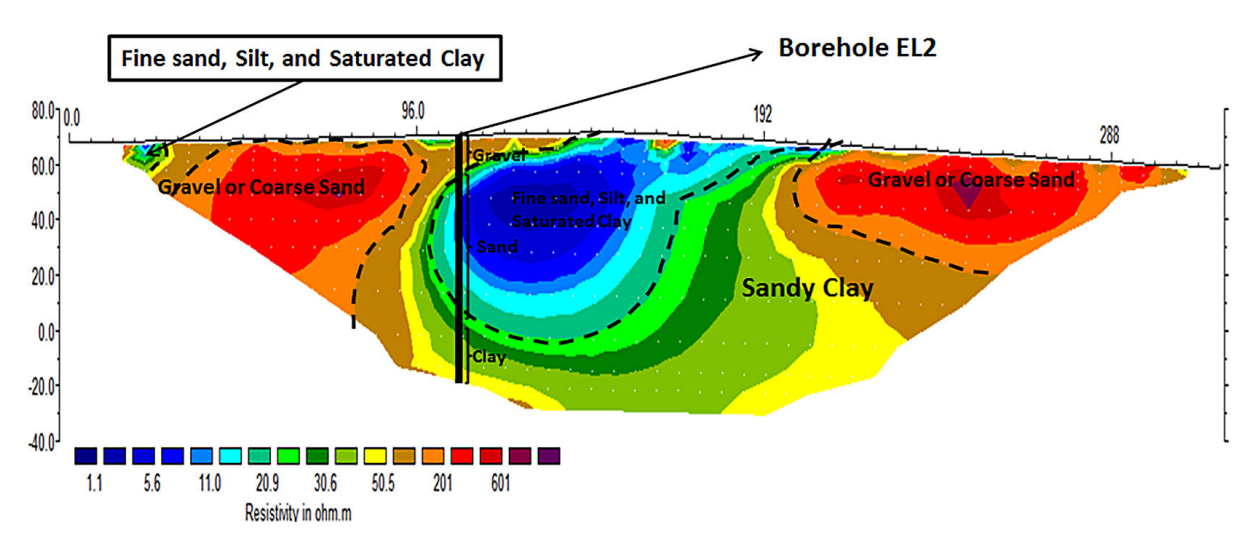


Figure 8. Cross-sectional representation of resistivity data 2 (R2) and electrical logging data 2 (EL2) at point D2

loading can reduce effective stress and trigger liquefaction. This condition is particularly critical in paddy field regions with shallow groundwater levels, where excess pore pressure buildup can damage irrigation systems, destabilize soils, and threaten nearby agricultural land and settlements in Pidie Jaya.

Jurong Ara (EL3 and R3)

The EL3 drilled well, located at Dayah Babul Istiqamatuddin, Jurong Ara Village, Jangka Buya District (5°13'35.60"N; 96°18'31.0"E), reached a depth of 122 m and revealed three main lithologies: sand, sandy clay, and clay (Figure 9). Sand layers are present at 0-19 m, 36-46 m, and 72–111 m, with resistivity values of $31–34 \Omega m$, indicating loose, water-saturated deposits that are highly susceptible to liquefaction under seismic loading. Sandy clay horizons occur at 19-26 m and 46–65 m, with resistivity values of 23–32 Ω m, representing partially consolidated units that retain substantial moisture and act as pathways for pore-pressure transmission. Clay layers are observed at 26-36 m, 65-72 m, and 111-122 m, with resistivity values of 23–33 Ω m, functioning as impermeable strata that confine groundwater within the sandy horizons.

This alternating stratigraphy of sand, sandy clay, and clay highlights critical liquefaction-prone conditions. Shallow sandy horizons, bounded by impermeable clay layers, provide favorable conditions for excess pore pressure development during seismic events. Environmentally, these subsurface characteristics pose significant risks

to agricultural lands, settlements, and local infrastructure in Jurong Ara Village, particularly during strong earthquakes.

The R3 resistivity profile, situated near rice fields in Jurong Ara Village (Figure 10), identifies three primary lithological units: sand, sandy clay, and clay. The shallow sand layer extends from 0–19 m, with resistivity values ranging from $0-57 \Omega m$. These unconsolidated, water-saturated sands are highly susceptible to liquefaction when subjected to seismic loading. Beneath this, sandy clay layers occur at depths of 4–34 m, exhibiting resistivity values of 0–23 Ω m. While partially cohesive, these horizons retain substantial moisture and can transmit excess pore water pressure upward during ground shaking. At greater depths, clay layers are observed from 15-40 m with resistivity values ranging from 13–750 Ωm, acting as aquitards that confine groundwater within the sandy strata.

This stratigraphic arrangement – loose sand confined by sandy clay and clay – forms a hydrogeological system that amplifies liquefaction susceptibility. Environmentally, the presence of these liquefiable sediments adjacent to agricultural areas poses risks such as soil instability, decreased crop productivity, and potential damage to irrigation networks and rural infrastructure during seismic events.

Environmental implications

The subsurface in Pidie Jaya consists of multiple lithological layers, each with distinct physical properties and transparency, influencing

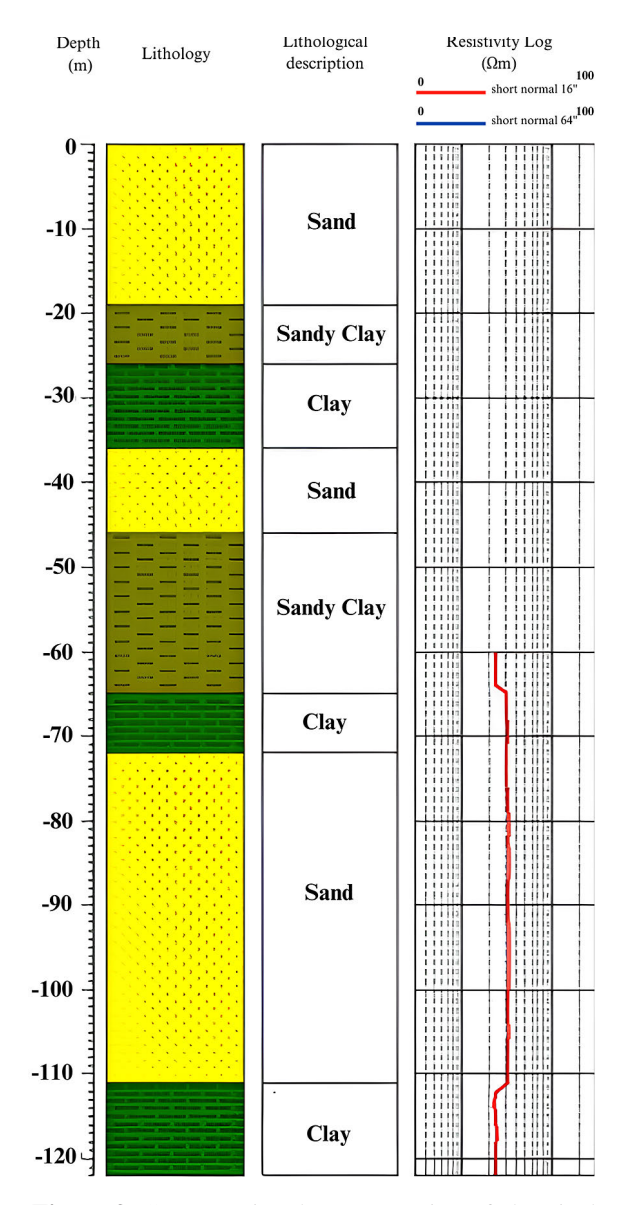


Figure 9. Cross-sectional representation of electrical logging data 3 (EL3) at point D3

groundwater retention, soil settlement, and stability. The topsoil is predominantly clay, characterized by low permeability and resistivity, functioning as a barrier that limits vertical groundwater movement while acting as a water retention unit. Beneath this clay layer lies a substantial sand-gravel aquifer, which provides significant groundwater storage and transport capacity due to its high permeability. Although these sand layers generally exhibit low resistivity, in some cases this may indicate finer-grained material or the presence of conductive pore fluids.

Below the sand-gravel aquifer, sandy clay layers act as aquitards with moderate resistivity and limited water transmission. The resistivity log curve of these layers shows a leftward trend, supporting their classification as semi-confining units. The hydrogeological system formed by clay (aquiclude) overlying sand-gravel (aquifer) and sandy clay (aquitard) facilitates groundwater storage and movement within the aquifer while restricting downward flow.

Geophysical and lithological data indicate that the study area is predominantly composed of unconsolidated sand and silt deposits, maintaining relatively uniform thickness across liquefaction-prone zones. In contrast, areas with different lithologies show reduced thickness gradients of loose sand and gravel, reflecting variability in depositional environments. Groundwater monitoring indicates shallow water tables consistently below 10 meters, with an average depth of 6.8 meters. This, combined with loose, saturated sand and silt deposits, indicates a high potential for liquefaction, as confirmed by electrical well logging and 2D resistivity imaging. The resistivity datasets show extensive low-resistivity zones from 0-49 meters depth, corresponding to loose sandgravel deposits, underlain by moderate-resistivity strata of sandstone from the Olim Formation and Alluvium Deposits.

Liquefaction is most likely in loosely packed, moderately saturated granular soils with poor drainage, such as silty sand, sand, and gravel. Under cyclic loading from seismic activity, these soils experience undrained deformation, volume reduction, increased pore water pressure, and decreased shear strength, leading to liquefaction (Seed and Idriss, 1971; Youd et al., 2001). The most susceptible formations are Holocene-aged deposits (≤10.000 years) with well-sorted, uniform grain sizes and full saturation, commonly found in river channels, coastal areas, sand dunes, and loess regions.

The geological composition of Pidie Jaya features alternating layers of sand, silt, clay, and sand-gravel deposits, interspersed with fragmented rock formations, reflecting tectonic activity, uplift, subsidence, and sedimentation. Groundwater depth varies from 1–4 meters in some areas and exceeds 4 meters near the Krueng Meureudu River. The aquifer system includes layers with varying permeability, where silt acts as a semi-permeable barrier and fine to coarse sand and sand-gravel layers serve as permeable pathways.

Overall, the high liquefaction risk is driven by shallow groundwater, unconsolidated granular soils, and cyclic loading, further amplified

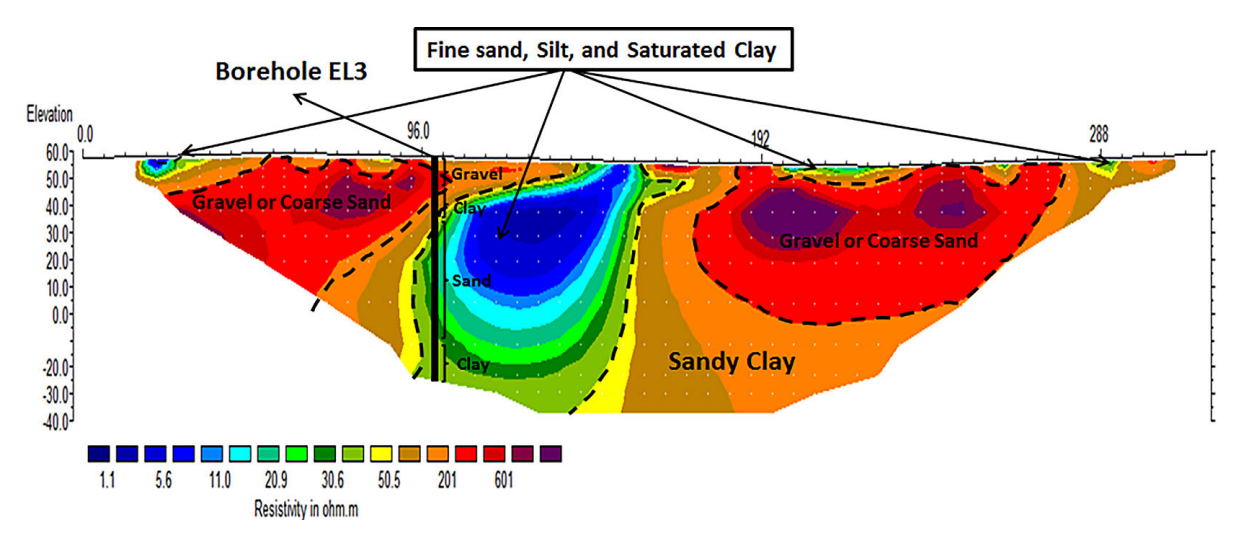


Figure 10. Cross-sectional representation of resistivity data 3 (R3) and electrical logging data 2 (EL2) at point D3

by active tectonics and Holocene deposits. The spatial continuity of these formations and their hydrogeological variability highlight the importance of comprehensive geotechnical and hydrogeological assessments to mitigate liquefaction hazards and support sustainable groundwater and environmental management.

CONCLUSIONS

The geophysical investigation using electrical well logging and 2D resistivity imaging in Pidie Jaya, Indonesia, reveals that the study area is dominated by unconsolidated sand, silt, clay, and sand-gravel deposits with a shallow groundwater table averaging 6.8 meters. The stratigraphic arrangement, including clay aquicludes, sand-gravel aquifers, and sandy clay aquitards, creates a hydrogeological system highly susceptible to liquefaction under cyclic loading, particularly during seismic events. Low-resistivity zones identified through 2D resistivity imaging correspond to loose, saturated sand-gravel deposits, confirming the high liquefaction potential in Holocene-aged sediments. The combination of unconsolidated granular soils, shallow groundwater, and active tectonic activity underscores the environmental and geotechnical risks in the region. These findings emphasize the need for comprehensive geotechnical and hydrogeological assessments to mitigate liquefaction hazards and promote sustainable management of groundwater resources and infrastructure planning.

Acknowledgements

The authors would like to thanks the Ministry of Educations, Culture, Research and Technology, Indonesia for financial support in the scheme of Penelitian Profesor-PTNBH USK 2023 Grant (Contract no. 70/UN11.2.1/PT.01.03/PNBP/2023). Special thanks are extended to technical staffs of geophysics laboratory, Geophysics and Physics student, Faculty of Engineering and Faculty of Sciences Universitas Syiah Kuala.

REFERENCES

- Aceh Energy and Mineral Resources Agency. (2019). Aquifer electrical logging data from boreholes in Pidie Jaya District, Aceh. Banda Aceh: Aceh Energy and Mineral Resources Agency. (Unpublished internal report)
- Amoroso, S., Rollins, K. M., Andersen, P., Gottardi, G., Tonni, L., Martínez, M. F. G., De Martini, P. M. (2020). Blast-induced liquefaction in silty sands for full-scale testing of ground improvement methods: Insights from a multidisciplinary study. *Engineering Geology*, 265, 105437. https://doi.org/10.1016/j.enggeo.2019.105437
- 3. Anda, S. T., Syukri, M., Fadhli, Z., Miftahunnisa, F. (2024). The implementation of conductivity data in delineating liquefaction zone in Banda Aceh and Aceh Besar, Indonesia. *AIP Conference Proceedings*, 3082(1), 040042. https://doi.org/10.1063/5.0202261
- Asmirza, M. S., Hidayat, A. M., Hakam, A., Hape, M. M. (2019). Liquefaction analysis of road embankment in Pidie Jaya due to Aceh earthquake in 2016. GEOMATE Journal, 16(57), 144–149. https:// doi.org/10.21660/2019.57.8141

- Ayadat, T. (2021). Assessment and identification of three types of difficult soils. *Acta Geodynamica* et Geomaterialia, 18(2). https://doi.org/10.13168/ AGG.2021.0015
- Bennett, J. D., Bridge, D. McC., Cameron, N. R., Djunuddin, A., Ghazali, S. A., Jeffery, D. H., Whandoyo, R. (1981). *Geologic map of the Banda Aceh quadrangle, Sumatra* [Systematic geological map]. Geological Research and Development Centre, Indonesia. https://geologi.esdm.go.id/geomap/pages/ preview/peta-geologi-lembar-banda-aceh-sumatera
- BMKG. (2016). Strong earthquake M=6.5 shakes Pidie Jaya, Aceh Province triggered by active fault activities [Press release]. https://www.bmkg.go.id/ press-release/?p=gempabumi-kuat-m6-5-guncangpidie-jaya-provinsi-aceh-dipicu-akibat-aktivitassesar-aktif
- 8. Duan, W., Congress, S. S. C., Cai, G., Zhao, Z., Pu, S., Liu, S., ... Chen, R. (2023). Characterizing the in-situ state of sandy soils for liquefaction analysis using resistivity piezocone penetration test. *Soil Dynamics and Earthquake Engineering*, *164*, 107529. https://doi.org/10.1016/j.soildyn.2022.107529
- 9. Harsono, A. (1997). Formation evaluation and log applications. Schlumberger Oilfield Services, Jakarta.
- 10. Jefferies, M., Been, K. (2016). *Soil liquefaction: A critical state approach* (2nd ed.). Taylor & Francis.
- 11. Kim, N., Park, G., Kim, S. Y., Lee, J. S., Park, J. (2023). Physics-inspired geophysical assessment of liquefaction potential in Pohang, South Korea. *Acta Geotechnica*, 1–15. https://doi.org/10.1007/s11440-023-02083-0
- 12. Kusumawardani, R., Chang, M., Upomo, T. C. (2021). Understanding of Petobo liquefaction flowslide by 2018.09.28 Palu-Donggala Indonesia earthquake based on site reconnaissance. *Landslides*, *18*, 3163–3182. https://doi.org/10.1007/s10346-021-01700-x
- 13. Lee, A., Oh, S., Kwon, H. (2023, September). Development of a 2D modified liquefaction potential index map using geophysical data in Pohang, Korea. In *NSG2023 29th European Meeting of Environmental and Engineering Geophysics* 2023, 1–5. European Association of Geoscientists & Engineers. http://dx.doi.org/10.2139/ssrn.4523452
- 14. Loke, M. H. (2004). *Tutorial: 2-D and 3-D electrical imaging surveys*. Retrieved from http://www.geotomosoft.com
- 15. Loke, M. H., Barker, R. D. (1996). Rapid least-squares inversion of apparent resistivity pseudosections by a quasi-Newton method. *Geophysical Prospecting*, 44(1), 131–152. https://doi.org/10.1111/j.1365-2478.1996.tb00142.x
- 16. Loke, M. H. (2010). *RES2DINV ver. 3.59 software manual*. Penang, Malaysia: Geotomo Software.

- 17. Dahlin, T., Zhou, B. (2004). A numerical comparison of 2D resistivity imaging with 10 electrode arrays. *Geophysical Prospecting*, *52*(5), 379–398. https://doi.org/10.1111/j.1365-2478.2004.00423.x
- 18. Binley, A., Kemna, A. (2005). DC resistivity and induced polarization methods. In Y. Rubin & S. S. Hubbard (Eds.), *Hydrogeophysics* 129–156. Springer. https://doi.org/10.1007/1-4020-3102-5 6
- 19. Mollica, R., de Franco, R., Caielli, G., Boniolo, G., Crosta, G. B., Motti, A., ... Castellanza, R. (2020). Micro electrical resistivity tomography for seismic liquefaction study. *Journal of Applied Geophysics*, *180*, 104124. https://doi.org/10.1016/j.jappgeo.2020.104124
- 20. Munirwan, R. P., Munirwansyah, M., Jamaluddin, K., Gunawan, H., Mubarak, A. Z., Ramadhansyah, P. J., Youventharan, D. (2020). Liquefaction potential analysis of reusep prestress bridge in Pidie Jaya due to 6.4 Mw earthquake. *IOP Conference Series: Materials Science and Engineering*, 712(1), 012010. https://doi.org/10.1088/1757-899X/712/1/012010
- 21. Muzli, M., Muksin, U., Nugraha, A. D., Bradley, K. E., Widiyantoro, S., Erbas, K., ... Wei, S. (2018). The 2016 Mw 6.5 Pidie Jaya, Aceh, North Sumatra, earthquake: Reactivation of an unidentified sinistral fault in a region of distributed deformation. Seismological Research Letters, 89(5), 1761–1772. https://doi.org/10.1785/0220180068
- 22. Qodri, M. F., Anggorowati, V. D. A., Mase, L. Z. (2022). Site-specific analysis to investigate response and liquefaction potential during the megathrust earth-quake at Banten Province Indonesia. *Engineering Journal*, 26(9), 1–10. https://doi.org/10.4186/ej.2022.26.9.1
- 23. Rastogi, B. K., Mohan, K., Sairam, B., Singh, A. P., Pancholi, V. (2022). Geotechnical, geological and geophysical investigations for seismic microzonation and site-specific earthquake hazard analysis in Gujarat. In *Advances in Earthquake Geotechnics* 73–91. Singapore: Springer Nature Singapore. https://doi.org/10.1007/978-981-19-3330-1_4
- 24. Ray, P., Sahu, R. B. (2021). Liquefaction potential along with pore water pressure generation of coastal sand of Digha in West Bengal, India. *Acta Geodynamica et Geomaterialia*, 18(2). https://doi.org/10.13168/AGG.2021.0012
- 25. Reynolds, J. M. (2011). An introduction to applied and environmental geophysics. John Wiley & Sons.
- Rusydy, I., Idris, Y., Mulkal, Muksin, U., Cummins, P., Akram, M. N., Syamsidik. (2020). Shallow crustal earthquake models, damage, and loss predictions in Banda Aceh, Indonesia. *Geoenvironmental Disasters*, 7, 1–16. https://doi.org/10.1186/s40677-020-0145-5
- 27. Sako, N., Fujii, M. (2019, June). Liquefaction evaluation using electric logging method for ground survey of a detached house. Paper presented at *The 29th*

- International Ocean and Polar Engineering Conference, Honolulu, Hawaii, USA. https://onepetro.org/ISOPEIOPEC/proceedings-abstract/ISOPE19/All-ISOPE19/ISOPE-I-19-567/21017
- Seed, H. B., Idriss, I. M. (1971). Simplified procedure for evaluating soil liquefaction potential.
 Journal of the Soil Mechanics and Foundations Division, 97(9), 1249–1273. https://doi.org/10.1061/ JSFEAQ.0001662
- 29. Syukri, M., Anda, S. T., Safitri, R., Fadhli, Z., Saad, R. (2020). Prediction of soil liquefaction phenomenon in Banda Aceh and Aceh Besar, Indonesia using electrical resistivity tomography (ERT). *GEOMATE Journal*, *18*(70), 123–129. https://doi.org/10.21660/2020.70.12814
- 30. Syukri, M., Taib, A. M., Fadhli, Z., Safitri, R. (2020). Geophysical investigation of road failure: The case of the main street of Alue Naga, Banda Aceh, Indonesia. *IOP Conference Series: Materials Science and Engineering*, 933, 012056. https://doi.org/10.1088/1757-899X/933/1/012056

- 31. ReliefWeb. (2016). *Indonesia: Earthquake Nov* 2016. https://reliefweb.int/disaster/eq-2016-000127-idn
- 32. Irhami, Munirwansyah, Sungkar, M. (2023, May). Study of liquefaction in the sand layer under the city of Banda Aceh against subduction earthquake source using Seed et al.(1976) and Castro (1975) methods. In *The 3rd Aceh International Symposium On Civil Engineering (Aisce)*: Towards The Sustainable And Green Construction Promoting Advanced Materials And Technology For Disaster Resilient Infrastructure And Environments 2711(1), 040001. AIP Publishing LLC. https://doi.org/10.1063/5.0149811
- 33. Youd, T. L., Idriss, I. M., Andrus, R. D., Arango, I., Castro, G., Christian, J. T., ... others. (2001). Liquefaction resistance of soils: Summary report from the 1996 NCEER and 1998 NCEER/NSF workshops on evaluation of liquefaction resistance of soils. *Journal of Geotechnical and Geoenvironmental Engineering*, 127(10), 817–833. https://doi.org/10.1061/(ASCE)1090-0241(2001)127:10(817)